JAST, Vol. 2, No. 4, pp 45–53

JAST
Journal of Aerospace Science and Technology

Transonic and Supersonic Overtaking of a Projectile Preceding a Shock Wave

H. Ahmadikia[1], E. Shirani[2]

In this paper, two-dimensional and axisymmetric, time dependent transonic and supersonic flows over a projectile overtaking a moving shock wave are considered. The flow is simulated numerically by solving full time averaged Navier-Stokes equations. The equations are linearized by Newton approach. The Roe's flux splitting method, second order central difference scheme for the diffusion terms and the second order approximation for time derivatives are used. For the turbulence terms, the Baldwin-Lomax and mixing length turbulence models are used. The present algorithm captures complicated features of flow including moving shock waves, expansion waves, boundary layers and wakes and their interactions. The results show that as the projectile passes through the moving shock wave, it changes the flow field features and pressure distribution dramatically. The drag force decreases and even becomes negative while the projectile takes over the shock wave. The flow features and the aerodynamic forces in transonic flow changes much more than those in the supersonic flow as the projectile passes through the shock wave. The results show that when the shock wave passes though the projectile, the flow field structures and the aerodynamic forces change abruptly. The drag force reduces and the shock wave passes through the projectile. Such variations are more vociferous for transonic flows than the supersonic flows. For transonic flows, the drag force changes sign and accelerates the projectile. Such behavior is important when the stability and control of the projectile are studied. Also such changes in pressure around the projectile and in the wake region change the projectile trajectory.

INTODUCTION

The aerodynamic characteristic of the flow, which is affected by the movement of a high-speed projectile overtaking a preceding shock wave from behind, is considered. This problem is a simplified version of a flow produced by high-speed projectile, which passes through a highly under expanded supersonic exhaust plume produced by the projectile while leaving a cylinder as shown in Figure (1). When the projectile passes through the moving shock wave, it moves form a high-pressure region, which is the flow behind the moving shock wave, to the region of lower pressure in front of the shock wave. Such cases are observed near the outlet of a ballistic range facility where a lunched projectile overtakes the blast movement produced by itself. Examples of such problems are the thruster, retro-rocket firings, silo injections, shock tunnel discharges, launching tube fired projectile, etc.

When a projectile overtakes the shock wave, complicated interaction of compression and expansion waves are produced. Therefore, the projectile experiences drastic changes in the aerodynamic forces that are applied to it. These changes highly affect the control and stability of the projectile. In fact, such a rapid change of aerodynamic forces may make the projectile unstable after the overtaking of the moving shock wave.

Most of the studies in this subject are derived from experimental observations and investigations [1, 2]. Since this phenomenon takes place in a very short

1. *Assistant Professor, Dept. of Mechanical Eng., Bou Ali Sina Univ., Hamadan, Iran, Email: ahmadikia@basu.ac.ir.*
2. *Professor, Dept. of Mechanical Eng., Isfahan Univ. of Tech., Isfahan, Iran, Email: eshirani@cc.iut.ac.ir.*

interval of time, the experimental measurements of the aerodynamic forces are extremely difficult in this period. Many researchers have considered the diffraction of a shock wave from objects like cylinder and sphere, i.e. see Reference [3], [4] and [5]. But in most cases, the object is stationary with respect to its surroundings. Wantanabe et al. [6] conducted a numerical study on the subsonic movement of a projectile while overtaking a preceding shock wave from behind. Wantanabe et al. [6] used three major assumptions in his paper. These are thin layer Navier-Stokes equation, Baldwin-Lomax turbulent model throughout the flow region and the first order approximation for the time derivative terms in the equations. The first two assumptions are not suitable for the wake region and the third assumption is not suitable for such a highly unsteady flow. A numerical study of shock wave induced by a supersonic projectile moving in a tube is described by Jiang et al. [7]. They used Euler equations with moving boundary conditions.

In this work, the movement of a projectile in a transonic and supersonic flow passing through a normal moving shock wave is investigated. For the transonic flows, the drag force is highly sensitive to the value of the flow Mach number. For example, it increases 100% when the free stream Mach number is increased from 0.95 to 0.97 [8]. To obtain such vast changes in aerodynamic forces, one needs to simulate the transonic flow with reasonable accuracy. Full Navier-Stokes equations are solved here to simulate axisymmetric and two-dimensional flows around a projectile.

The present study aims at understanding on wave dynamic process occurring in overtaking flows at the projectile launching stage to demonstrates the unsteady flow phenomena and to provide useful information for the research on the ram accelerator and on the gun firing problem. The flow structures, pressure distributions and drag forces are obtained as a function of time while the projectile passes through the moving shock wave.

FLOW FEATURES

The flow field, the projectile and the preceding shock wave, which are considered in this paper, are schematically shown in Figure 2. In this figure, U_s, U_p and u_2 are absolute velocities of the shock wave, projectile and flow behind the shock wave, respectively. If the projectile's absolute motion is supersonic, then depending on the value of the relative velocity of the projectile, its motion with respect to the flow behind the shock wave can be subsonic, sonic or supersonic. Flow features relative to the projectile are shown in Figure 3. In this figure, the projectile is assumed to be stationary. The relative velocities of the flow and shock wave are shown.

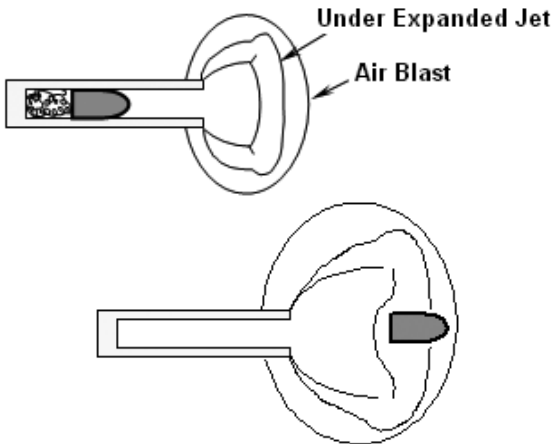

Figure 1. Schematic of the flow features for a projectile passing through a self-produced plume

The relations between the flow properties for the moving shock wave are as follows [4]:

$$\frac{p_2}{p_1} = \frac{2\gamma M_s^2 - (\gamma - 1)}{(\gamma + 1)}, \tag{1}$$

$$\frac{\rho_2}{\rho_1} = \frac{\Gamma\,(p_2/p_1) + 1}{\Gamma + p_2/p_1}, \tag{2}$$

$$\frac{u_2}{c_1} = M_s \left[1 - \frac{(\gamma - 1)M_s^2 + 2}{(\gamma + 1)M_s^2}\right], \tag{3}$$

$$\frac{c_2}{c_1} = \sqrt{\frac{p_2}{p_1}\frac{\rho_1}{\rho_2}}, \tag{4}$$

where, $\Gamma = (\gamma + 1)/(\gamma - 1)$ and $c = (\gamma p/\rho)^{1/2}$. M_s is the absolute value of the shock Mach number, p, ρ, γ and c are the pressure, density, specific heat ratio and speed of sound, respectively. The states (1) and (2) are the locations ahead and behind the moving shock wave, respectively. Assuming M_{p0} is the absolute projectile Mach number and M_{p2} is the relative projectile Mach number with respect to the flow behind the shock wave, then:

$$M_{p0} = M_{p2}\left(\frac{c_2}{c_1}\right) + \frac{u_2}{u_1}, \tag{5}$$

where, $M_{p0} = U_P/c_1$ and $M_{p2} = (U_P - u_2)/c_2$. Since M_s is known, u_2/u_1 and c_2/c_1 can be obtained from Eqs. (3) and (4). Although the projectile Mach number with respect to the ground M_{p0}, is greater than one, the flow over the projectile can be subsonic, M_{p2} <1 or supersonic, M_{p2}>1.

Mach number relations behind the preceding shock wave for the region of subsonic or transonic overtaking are shown in Figure 4. This figure is obtained by inserting M_{p2}=1 in Eq. (5). If M_{p0} is either above the solid line or between the lines, supersonic or subsonic overtaking will take place, accordingly. If M_{p0} is under the dashed line, the projectile does not take over the

shock wave. In Figure 5, M_{p2} is plotted against M_{p0} for various shock Mach numbers. This plot is obtained using Eqs. (3) to (5).

GOVERNING EQUATIONS AND NUMERICAL METHODS

The full Navier-Stokes governing equations of two-dimensional and axisymmetric unsteady flows are given by:

$$\frac{\partial \vec{Q}}{\partial \tau}+\frac{\partial \vec{E}_i}{\partial x}+\frac{\partial \vec{F}_i}{\partial y}=\frac{\partial \vec{E}_v}{\partial x}+\frac{\partial \vec{F}_v}{\partial y}+\vec{H}, \tag{6}$$

where,

$$\vec{Q}=y^m\begin{bmatrix}\rho\\ \rho u\\ \rho v\\ e_t\end{bmatrix},\qquad \vec{E}_i=y^m\begin{bmatrix}\rho u\\ \rho u^2+p\\ \rho uv\\ (e_t+p)\,u\end{bmatrix},$$

$$\vec{F}_i=y^m\begin{bmatrix}\rho v\\ \rho uv\\ \rho v^2+p\\ (e_t+p)\,v\end{bmatrix},\qquad \vec{E}_v=y^m\begin{bmatrix}0\\ \tau_{xx}\\ \tau_{xy}\\ u\tau_{xx}+v\tau_{xy}+\dot{q}_x\end{bmatrix},$$

$$\vec{F}_v=y^m\begin{bmatrix}0\\ \tau_{yx}\\ \tau_{yy}\\ u\tau_{xy}+v\tau_{yy}+\dot{q}_y\end{bmatrix},\qquad \vec{H}=\begin{bmatrix}0\\ 0\\ m\,(p-\tau_{\theta\theta})\\ 0\end{bmatrix},$$

$$p=(\gamma-1)\left[e_t-(1/2)\,\rho\left(u^2+v^2\right)\right],$$

$$\tau_{xx}=(\lambda+2\mu_{eff})\,\frac{u}{x}+\lambda\left(\frac{v}{y}+m\frac{v}{y}\right),$$

$$\tau_{xy}=\mu_{eff}\left(\frac{u}{y}+m\frac{v}{y}\right),$$

$$\tau_{yy}=(\lambda+2\mu_{eff})\,\frac{v}{y}+\lambda\left(\frac{v}{x}+m\frac{v}{y}\right),$$

$$\tau_{\theta\theta}=(\lambda+2\mu_{eff})\,\frac{v}{y}+\lambda\left(\frac{u}{x}+\frac{v}{y}\right),$$

$$\dot{q}_x=-(k+k_t)\,\frac{\partial T}{\partial x},\ \dot{q}_y=-(k+k_t)\,\frac{\partial T}{\partial y},$$

$$\mu_{eff}=\mu+\mu_t,\qquad k_t=\mu_t c_p/Pr_t,$$

$$Pr_t=0.9,\qquad \lambda=-\frac{2}{3}\mu, \tag{7}$$

where u and v are velocity components, e_t is total internal energy and T is temperature. m is equal to one for axisymmetric flow, and zero for two-dimensional flows. μ, μ_t, k and k_t are molecular and turbulent viscosities and thermal conductivities, respectively. The governing equations are transferred into a body fitted coordinate system and are solved numerically. The Baldwin-Lomax [9] algebraic two-layer turbulence model is used for flow around the projectile and an

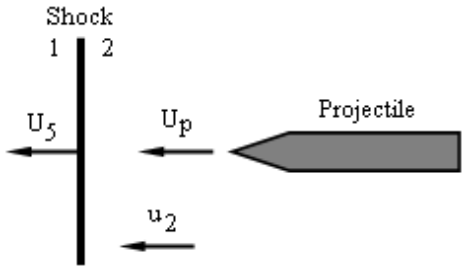

Figure 2. Flow configuration with absolute velocities

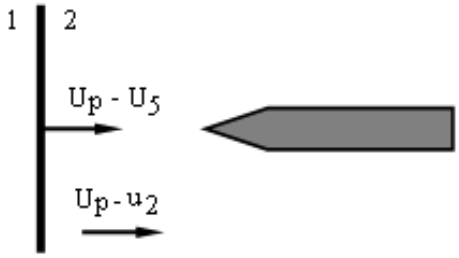

Figure 3. Flow configuration with relative velocities

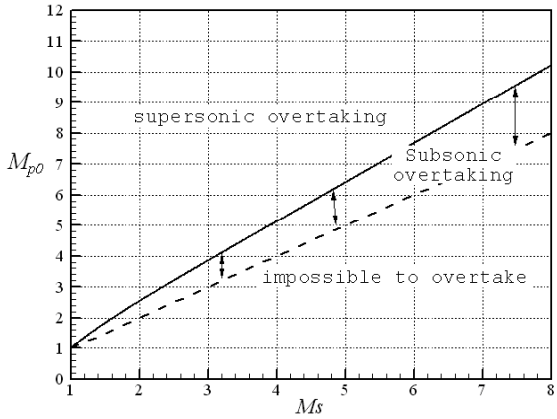

Figure 4. Projectile Mach number as a function of the shock Mach number

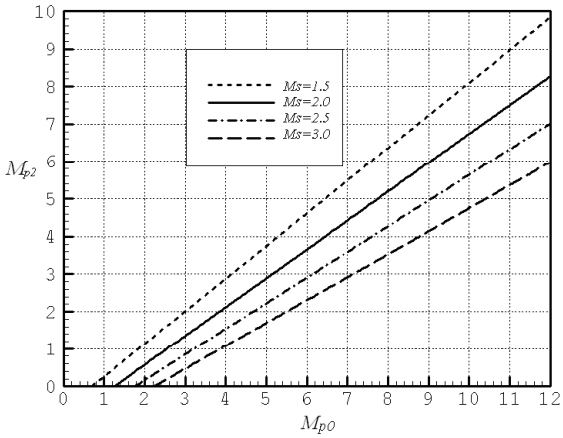

Figure 5. Relative projectile Mach number as a function of projectile Mach number

algebraic mixing length model intoduced by Vatssa et al. [10] is used for flow in the wake region. At the intersection of the two region, the eddy viscosity is obtained by assuming linear variation from one region to another. Also for the flows behind the projectile, where it is affected by both boundary layer and the wake region, the average values of the eddy viscosity is used.

The equations of motion are linearized using Newton approach. The convective fluxes are approximated by Roe's flux-splitting method [10,11], and the diffusion fluxes are approximated by the second order central difference scheme. The time derivatives are approximated by the second order backward difference scheme. To prevent entropy deflection around the sonic line, Harten and Hyman [13] entropy conditions are implemented. The minimum of two-gradient limiter is also employed to prevent numerical oscillations. For the two-dimensional flow, instead of half flow field by symmetry, the whole flow feild is simulated.

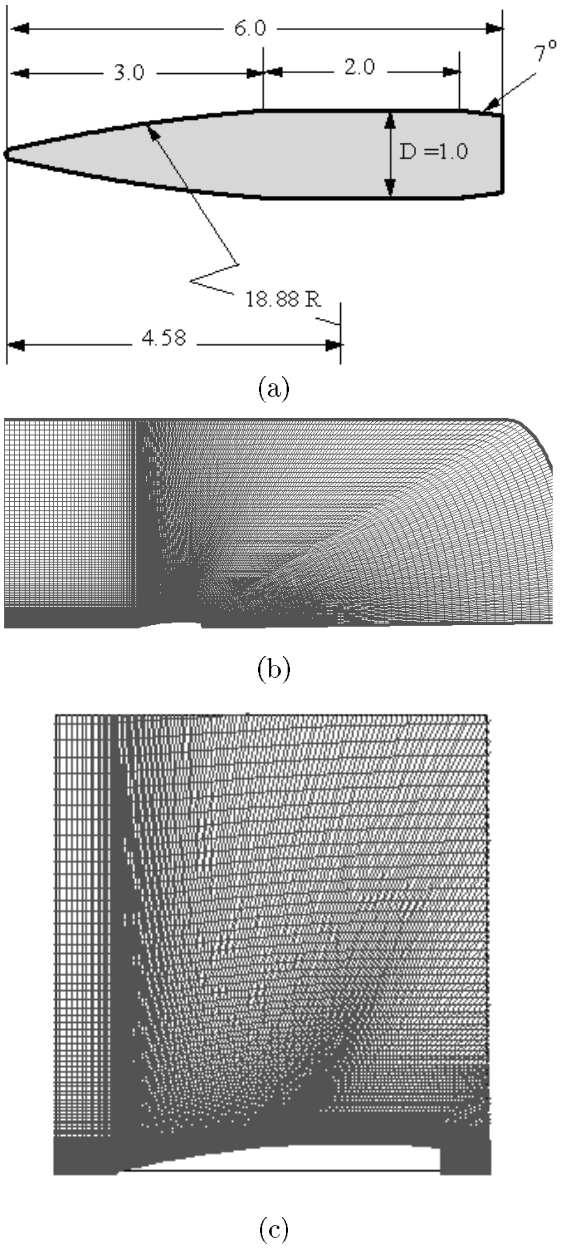

Figure 6. Grid configuration for transonic axisymmetric flows, (a) Projectile geometry, (b) Grid for whole domain, (c) Grid close to the projectile.

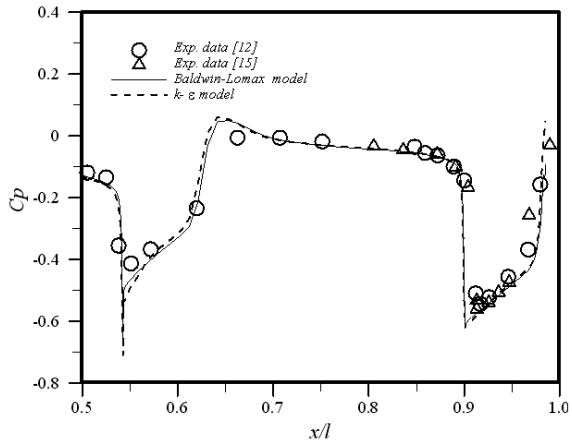

Figure 7. Pressure distribution on the projectile surface for steady state case, M_{p2}=0.94

INITIAL CONDITIONS

In order to specify the initial boundary conditions, the initial location of the moving shock wave must be chosen. Suitable initial position of the moving shock wave with respect to the projectile depends on the flow conditions. If subsonic or transonic overtaking is considered, the initial position of the incident shock wave must be located at a location far enough from the projectile so that the effects of projectile on the flow can be calculated correctly (Figure 3). In this case, the CPU time required to solve the problem is very large, as will be indicated later. The initial conditions at the front of shock wave (state 1 on Figure 2) are obtained according to Eqs. (1) to (3). To obtain the initial flow field over the projectile, the steady flow around it is numerically solved by using the flow condition behind the shock wave as free stream conditions.

GRID GENERATION

The accuracy and efficiency of numerical solutions depend considerably on the quality of the grid employed. In this work, H-type structure grid is used. The SOCBT (Secant-Ogive-Cylinder-Boat Tail) geometry is used for the projectile [14]. For axisymmetric case the number of grid points along the projectile is 300 and along the normal direction to the projectile is 110. For the supersonic axisymmetric case, the solution domain is 40 percent smaller than that of transonic case because in this case the distance in front of the body could be chosen to be smaller. For two-dimensional

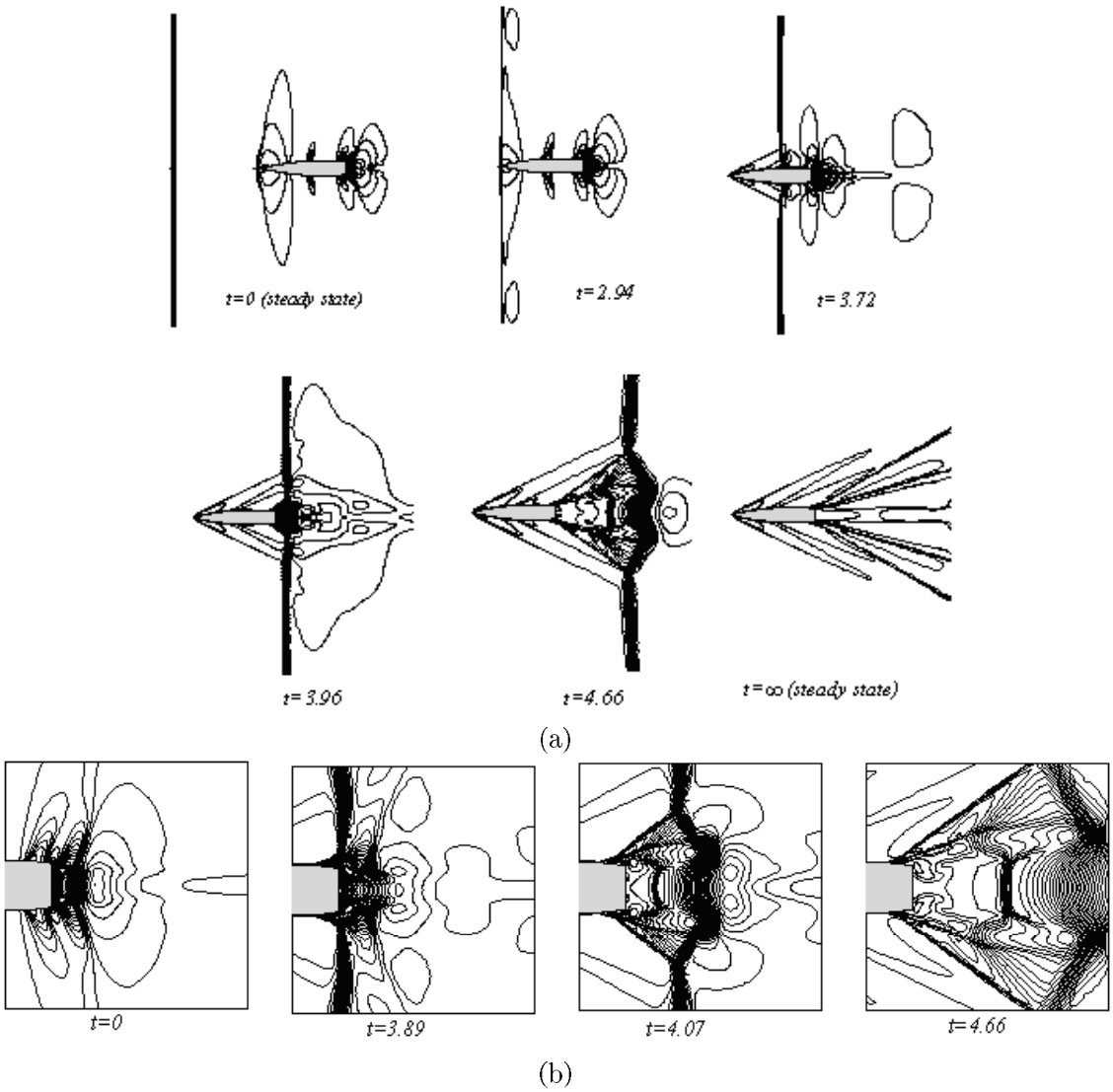

Figure 8. Flow features and density contours, as the projectile overtakes the shock wave, M_{p2}=0.94, (a) Total region, (b) Wake region.

flows, the O-type grid is used. The number of grid nodes along the body is 400 and normal to the body is 110. In this case, the solution domain is 30 percent greater than the axisymmetric case.

RESULTS

A computer code was developed and validated for several test cases to test the accuracy of the code, [15] and [16]. Also the diffraction of a normal shock wave with a cylinder and sphere are simulated and compared with experimental data [5].

The shock Mach number M_s for both two-dimensional and axisymmetric cases is 2. According to Eqs. (2) to (5), or Figures (4) and (5), when $2<M_{p0}<2.55$, the flow over the projectile is subsonic and when $M_{p0}>2.55$, it is supersonic. Two values of M_{p0}, i.e., 2.47 and 3.07, are chosen which correspond to M_{p2}=0.94 and 1.4, respectively. The results for transient axisymmetric and two-dimensional cases are presented here. First, the results for transonic axisymmetric flow, then supersonic axisymmetric flow and finally two-dimensional flow are presented.

Figure (6) shows the projectile geometry and the computational grid for transonic axisymmetric case. The SOCBT geometry is used for the projectile [14]. Here, $\Delta y_{min}/d=4.1\times 10^{-3}$ and $\Delta s_{min}/d=5.4\times 10^{-3}$ where y is normal to the body, d is the projectile diameter and s is the arc length of the grid along the projectile surface. Figure 7 shows surface pressure distributions at the steady state solution which is needed as an initial condition for the axisymmetric transonic case, M_{p2}=0.94. The results are obtained for both the k-ϵ and Baldwin-Lomax models. As

mentioned earlier, the mixing length model is used for the wake region and the average value obtained from the two models is used for the intersection region.

In this figure, the pressure is compared with experimental data [14] and [17] and good agreement is obtained. As it is shown, both k-ϵ and Baldwin-Lomax models give similar results. Therefore, we have chosen the Baldwin-Lomax model to simulate the flow field in this paper. Finally to the knowledge of the authors, there are no quantitative experimental results for the transient case to be compared with. So in this paper only the steady state solution is compared with the experimental data.

Figure (8) shows the sequence of the flow configurations developed for transonic flow with M_{p2}=0.94 around the projectile overtaking the preceding shock wave. In this figure, time is normalized by $l/U_{1\infty}$, where l is the projectile length. The density contours are shown at various time steps in this figure.

When the shock wave passes through the projectile nose, it is reflected, and the shock waves and reflected waves move along the projectile axes (Figure 8a, t=2.94). As the shock wave moves downstream (at t=3.72), the angle between the two waves is decreased until a Mach effect is formed. Then a new shock wave, the Mach shock, is formed (t=4.66). At this stage, the triple point, which is the location at the intersection of the three shock waves, moves downstream and a slipstream and certain vortices are produced. As the incidence shock wave moves downstream, fisrt interacts with boundary layers and then with the expansion waves at the boat tail of the projectile and its shape is changed, Figure (8b). As shown in the figure, the base corner vortices are produced at the edge of the projectile back and move downstream. Also the shock wave interacts with the wake behind the body, which forms a complicated phenomenon. Finally, the shock wave moves downstream and away from the body until a steady state solution is eventually obtained. During this period, the flow structure around the body does not change much.

In Figure 9, the velocity vectors, streamlines and the density contours at the wake region are shown. When the shock wave moves through the wake region, it interacts with the vortices separated from the body. Then a new vortex is formed at the edge of the body as the previous vortex is separated from it, see Figure 9. As shown in the figure, the vortex ring is formed due to the strong reverse flow at the wake region. As a result, the impinging shock wave is formed between the base and the vortex ring. Thus, a rear shock wave between the vortex ring and the back of the body is formed. The induced flow at the back of the body turns toward the edge of the body and the corner vortex is formed due to the separation of flow at the edge of the body.

Figure (10), shows the density contours at different time steps for M_{p2}=1.4. In this case, the supersonic overtaking has taken place. Here, the behavior of the moving shock wave is studied in presence of the oblique shock wave formed in front of the body due to the supersonic nature of the flow. The shock wave is affected as a result of such collision, and the shock angle

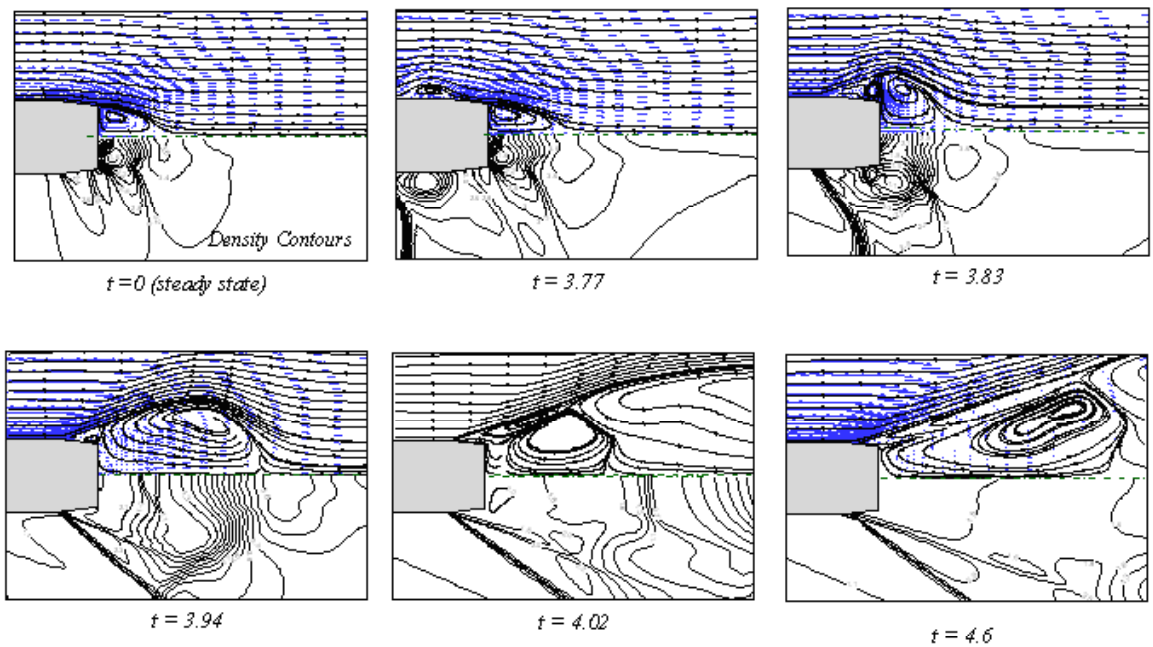

Figure 9. Velocity Vectors, streamlines and density contours, as the projectile overtakes the shock wave, M_{p2}=0.94 at different times.

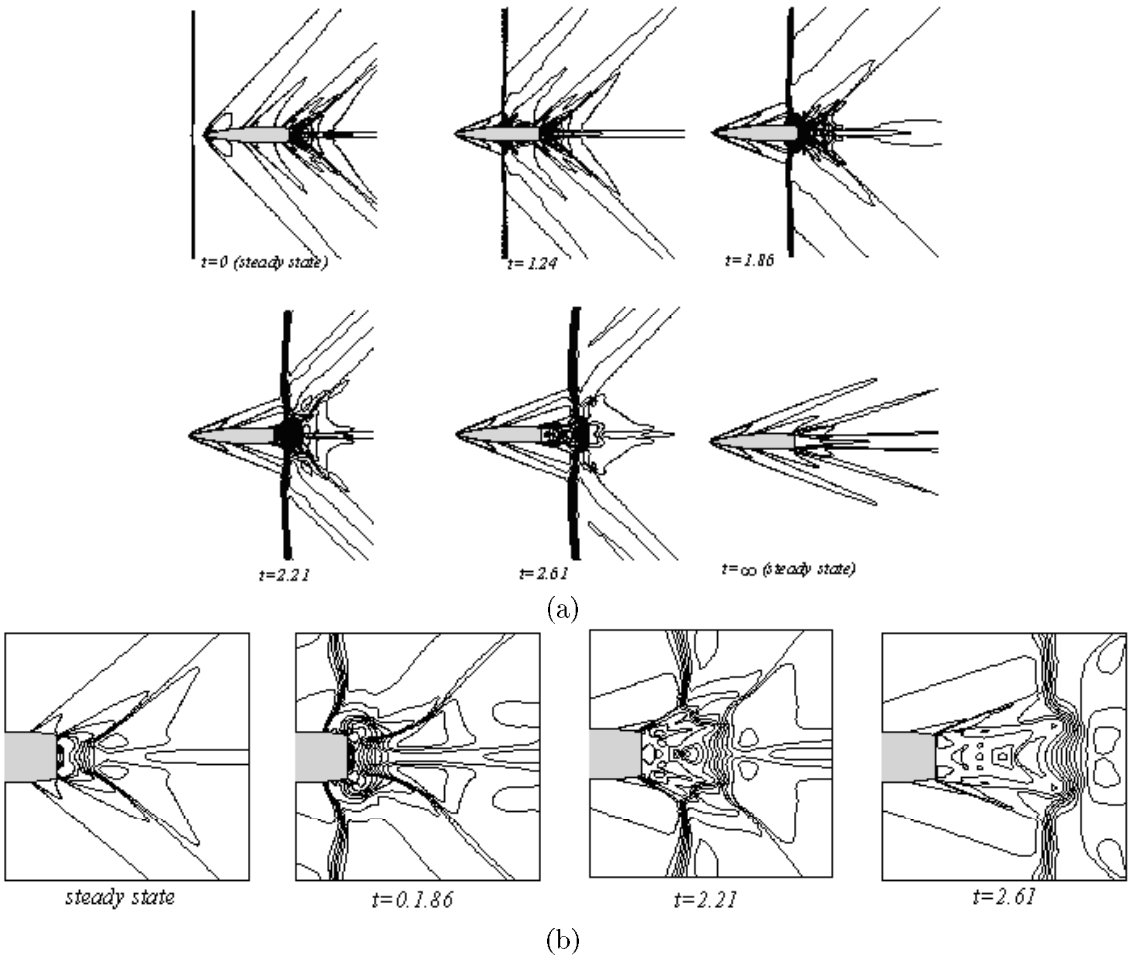

Figure 10. Flow features and density contours, as the projectile overtakes the shock wave, M_{p2}=1.4, (a) The whole region, (b) The wake region.

becomes smaller. The diffracted wave interacts with the expanded waves formed on the projectile tail edges. Then it interacts with the wake region and moves further downstream until the steady state solution is obtained.

Figures (11) and (12) show the pressure distribution at different time steps for the transonic and supersonic axisymmetric flows, respectively. In these figures, the pressure coefficient is defined as $Cp = (p/p_2 - 1)/(0.5\gamma M_2^2)$. As the projectile passes through the moving shock wave, it moves from the high-pressure region to the low-pressure region. As a result of vortex-shock wave interactions, the pressure on the projectile surface near the shock wave changes considerably. It is especially important to know, when the flow is supersonic compared to the supersonic flow. The pressure distribution does not change after the shock waves move downstream away from the body. The pressure is constant for t>1.2ts, and 6.5ts for supersonic and transonic cases, respectively.

The drag coefficient and the effect of grid size for the transition case are shown in Figure 13. The drag coefficient is nearly constant before the projectile reaches the shock wave. But as soon as it reaches the shock waves, the drag force decreases suddenly and even becomes negative. In this case, not only is the pressure drag not against the projectile movement, it accelerates the projectile. This is due to the sudden partial decrease of the pressure of the projectile surface that has passed through the shock wave. Even after the shock wave passes through the whole body, the drag force is still negative. It takes some time before the flow becomes steady and the effects of the shock wave in the flow field disappear.

Figure 14 shows the drag coefficient for supersonic overtaking, when M_{p2}=1.4. In this case, the drag force is constant until the shock wave reaches the nose of the body as expected. As the shock wave moves along the projectile axis, the drag force decreases and becomes as low as - 0.2. But after the shock wave leaves the projectile, its effects on the flow field vanish and the drag force increases again and reaches its steady state value, 0.19. For transonic flows, the changes are much more than for the supersonic flow. Also it takes

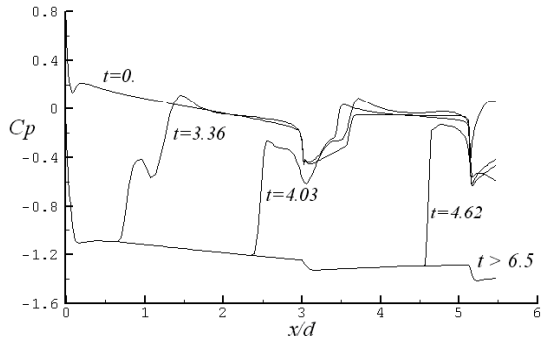

Figure 11. Pressure distribution for transonic axisymmetric cases.

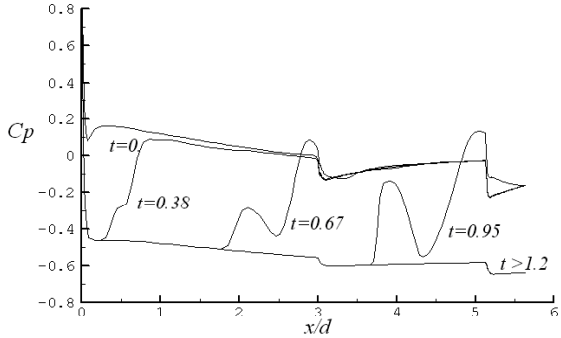

Figure 12. Pressure distribution for supersonic axisymmetric cases.

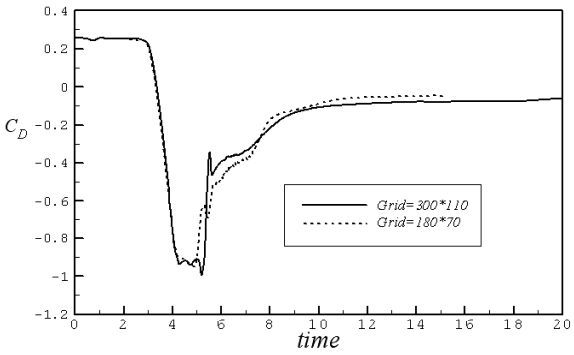

Figure 13. Drag coefficient as a function of time for transonic axisymmetric case.

more time for transonic flow to reach the steady state condition compared to the supersonic case. The drag coefficient reaches 0.18 as the flow becomes steady.

The effect of the grid size on the drag coefficient is shown in Figure (14). As shown, for the grid sizes examined, no significant effect on the qualitative behavior of the drag coefficient history is observed.

The drag coefficient for the two-dimensional transonic flow is shown in Figure 15. In this case, the shock wave and vortices are stronger than the previous cases. Thus, the variation of the drag coefficient is larger. As the projectile moves toward the shock wave, the drag coefficient is nearly constant, but it suddenly decreases when the projectile reaches the shock wave.

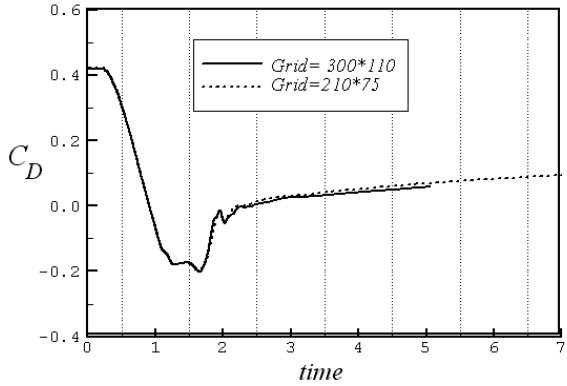

Figure 14. Drag coefficient as a function of time for supersonic axisymmetric case.

Due to the vortex shedding on the projectile tail and its interaction with the shock wave, some changes in the drag coefficient are observed and the drag coefficient finally reaches its steady state value at lerger times, after the projectile passes through the shock wave.

Figure (16) shows the drag coefficients for supersonic overtaking of a two-dimensional projectile. Compared to the transonic case, the variation of the drag coefficient with respect to time is smaller as shown in the figure. The reason is that in this case, the vortex shedding in the wake region is much smaller. In this case, the drag coefficient does not reach a negative value as in the case of the axisymmetric problem.

CONCLUSION

In this paper, it is shown that the numerical solution of Navier-Stokes equations using the control volume approach and the Reimann Roe flux splitting method with a minimum of two-gradient limiter and the Harten-Hayman entropy condition is capable of simulating the transient motion of the flow with a projectile overtaking a moving shock wave for both transonic and supersonic overtaking and also two-dimensional and axisymmetric bodies. Complicated features of the flow are captured and the drag coefficient is shown to change drastically when the projectile passes through the moving shock wave. The computed results show the transition of the flow field from transonic to supersonic, which is an inherent property of transonic overtaking. The most distinctive phenomenon is that there exists a strong adverse pressure gradient in the axisymmetric case, and the boundary layer separation is observed. The configuration and the formation of interaction flow field between the overtaken vortex ring and the projectile base are clarified. The effects of the overtaking on the flow features and the aerodynamic forces in transonic case are much more than the supersonic case. For axisymmetric flows, the drag force becomes negative and the projectile is pushed forward by the pressure drag.

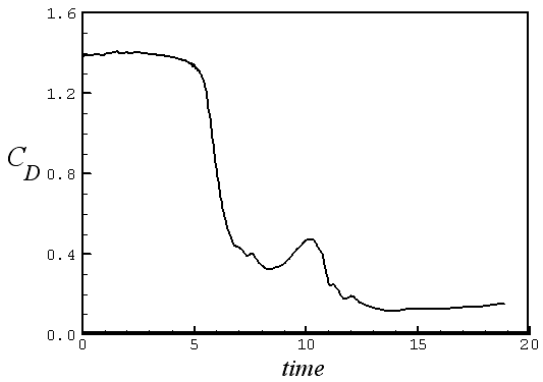

Figure 15. Drag coefficient as a function of time for transonic 2-D case.

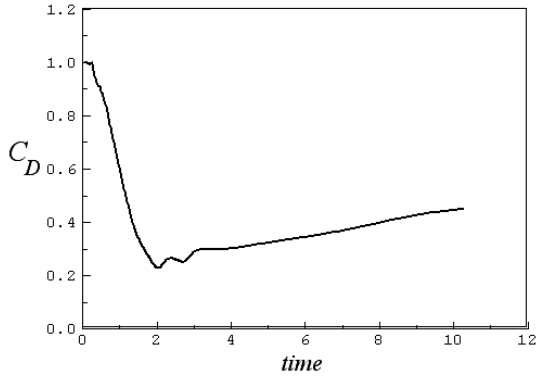

Figure 16. Drag coefficient as a function of time for supersonic 2-D case.

REFERENCES

1. Schmidt, E. M. and Shear, D. D., "Optical Measurements of Muzzle Blast", *AIAA Journal*, **13**(8), PP 1086-1091(1975).
2. Erods, J. I. and Del Guidice, P. D., "Calculation of Muzzle Blast Flow Fields", *AIAA Journal*, **13**(1), PP 1048-1055(1975).
3. Bryson, A. E., Gross, R. W. F., "Diffraction of Strong Shocks by Cones, Cylinders and Spheres", *Journal of Fluid Mechanics*, **10**(1), PP 1-16(1961).
4. Yang, J. Y., Liu, Y. and Lomax, H., "Computation of Shock Wave Reflection by Circular Cylinder", *AIAA Journal*, **25**(5), PP 683-689(1987).
5. Shirani , E. and Ahmadikia, H., "The Diffraction of Shock Waves over a Cylinder and a Sphere Using Roe[s Scheme", The Eighth Asian Congress of Fluid Mechanics, Shenzhen, China, PP 417-421(1999).
6. Wantanabe, P., Fujii, K. and Higashino, F., "Three Dimensional Flow Computation Around a Projectile Overtaking a Preceding Shock Wave", *Journal of Spacecraft and Rockets*, **35**(5), PP 619-625(1998).
7. Jiang, Z., Yonghui, H., and Takayama, K., "Shocked Flows Induced by Supersonic Projectiles Moving in Tubes", *Computers and fluids*, **33**, PP 953-966(2004).
8. Nietubicz, C. J., "Navier-Stokes Computations for Conventional and Hollow Projectile Shapes at Transonic Velocities", *AIAA Paper 81-1262*, Palo Alto Calif, (1981).
9. Baldwin, B. S. and Lomax, H., "Thin Layer Approximation and Algebraic Model for Separated Turbulent Flow", *AIAA Paper*, PP 78-257(1978).
10. Vatsa, V.V., and et al, "Solution of Slightly Underexpanded Two Dimensional and Axisymmetric Coflowing Jets", *AIAA Journal*, **18**, PP 303-310(1981).
11. Roe, P. L., "Characteristic-Based Schemes for the Euler Equations", *Annual Review of Fluid Mechanics*, **18**, PP 337-365(1986).
12. Roe, P. L., "The Use of the Riemann Problem in Finite Difference Schemes", *Lecture Notes in Physics*, **141**, PP 354-359(1981).
13. Harten, A. and Hyman, J. M., "Self Adjusting Grid Methods for One-Dimensional Hyperbolic Conservation Laws", *Journal of Computational Physics*, **50**, PP 235-269(1983).
14. Nietubicz, C. J., Inger, G. R. and Danberg, J. E., "A Theoretical and Experimental Investigation of a Transonic Projectile Flow Field", *AIAA Journal*, **22**(1), PP 35-41(1984).
15. Ahmadikia, H. and Shirani, E., "Assessment of Roe's Riemann Solver in Hypersonic 2-D and Axisymmetric Blunt Body Flows", Iran, Isfahan University of Technology, Esteghlal, **11**, (2001).
16. Ahmadikia, H., Shirani, E, "Transonic Flow over a Projectile Using k-ϵ Turbulence Models", Proceedings of The Third Aeronautical Engineering Conference, Tehran, Iran, (2000).
17. Cheing. C. C. and Danberg, J. E., "Navier-Stokes Computations Transonic Projectile at Angle of Attack and Comparison with Experimental Data", *AIAA Paper*, PP 88-2584(1988).